Mass of the higgs versus fourth generation masses

V.A. Novikov*, L.B. Okun†,
ITEP, Moscow, Russia
A.N. Rozanov‡,
CPPM, IN2P3, CNRS, Univ. Mediteranee, Marseilles, France
and ITEP, Moscow, Russia
M.I. Vysotsky§
ITEP, Moscow, Russia

Abstract

The predicted value of the higgs mass m_H is analyzed assuming the existence of the fourth generation of leptons (N, E) and quarks (U, D). The steep and flat directions are found in the five-dimensional parameter space: m_H, m_U, m_D, m_N, m_E. The LEPTOP fit of the precision electroweak data is compatible (in particular) with $m_H \sim$ 300 GeV, $m_N \sim 50$ GeV, $m_E \sim 100$ GeV, $m_U + m_D \sim 500$ GeV, and $|m_U - m_D| \sim 75$ GeV. The quality of fits drastically improves when the data on b- and c-quark asymmetries and new NuTeV data on deep inelastic scattering are ignored.

It is well known that in the framework of Standard Model the fit of electroweak precision data results in prediction of light higgs, the central value of its mass being lower than the direct lower limit set by LEP II [1]. One possible way to raise the predicted value of m_H is to assume the existence of

*email: novikov@heron.itep.ru
†email: okun@heron.itep.ru
‡email: rozanov@cppm.in2p3.fr
§email: vysotsky@heron.itep.ru

fourth generation of leptons and quarks, [2, 3] . Implications of extra quark-lepton generations for precision data were studied in a number of papers [2] - [7]. Leptons of fourth generation (E,N) should be very weakly mixed with the ordinary ones, while in quark sector (U,D) mixing is limited only by unitarity of 3×3 CKM matrix. In particular it was noticed in ref. [2] that the predicted mass of the higgs could be as high as 500 GeV. That conclusion was based on a sample of 10.000 random inputs of masses of fourth generation leptons and quarks. However the sets of the lepton and quark masses were presented independently (see Fig. 7 in ref. [2]). Thus it is not clear how they were combined.

In this letter we try to develop a systematic approach to the problem by using our LEPTOP code [8] to find steep and flat directions in the five-dimensional parameter space: m_H, m_U, m_D, m_E, m_N. For each point in this space we perform three-parameter fit $(m_t, \alpha_s, \bar{\alpha})$ and calculate the χ^2 of the fit. It turns out that the $\chi^2_{\rm min}$ depends weakly on $m_U + m_D$ and m_H, while its dependence on $m_U - m_D$, m_E and m_N is strong. We limit ourselves to the values of m_N larger than 50 GeV because according to experimental data from LEP II on the emission of initial state bremsstrahlung photons, $m_N > 50$ GeV at 95% c.l. [9, 10].

We analyzed Summer 2001 precision data (ref. [1] which are also given in the Table 1 in ref. [3]). Figures 1-4 show $\chi^2_{\rm min}$ (crosses) and constant χ^2 lines corresponding to $\Delta\chi^2 = 1, 4, 9, 16, ...$ on the plane $m_N, m_U - m_D$ for fixed values of $m_U + m_D = 500$ GeV, $m_H = 120$ (Figs. 1 and 3) and 500 GeV (Figs. 2 and 4) and $m_E = 100$ (Figs. 1 and 2) and 300 GeV (Figs 3 and 4). We also performed fits for $m_H = 300$ GeV.

The above choice of masses is based on a large number of fits covering a broad space of parameters: 300 GeV $< m_U + m_D <$ 800 GeV; 0 GeV $< m_U - m_D <$ 400 GeV; 100 GeV $< m_E <$ 500 GeV; 50 GeV $< m_N <$ 500 GeV; 120 GeV $< m_H <$ 500 GeV. Concerning quarks, $m_U + m_D$ is bounded from below by direct searches limit, while from above by triviality arguments. Since χ^2 dependence on $m_U + m_D$ is very weak, our choice of intermediate value $m_U + m_D = 500$ GeV represents a typical, almost general case. For this choice $|m_U - m_D|$ can not be larger than ~ 200 GeV because of the mentioned above direct searches bound.

Concerning charged lepton, its mass is taken above LEP II bound. We present fits at two values of m_E (100 GeV and 300 GeV) and one can see how fit is worsening with m_E going up.

Concerning the value of m_H, we vary it from the lower LEP II limit up to triviality bound and since the dependence of observables on m_H is flat, one can get χ^2 behaviour from two limiting points: m_H =120 and 500 GeV.

For $m_E = 100$ GeV we have the minimum of χ^2 at $m_N \simeq 50$ GeV and:

$$
\begin{array}{lll}
\text{for } m_H = 120 \text{ GeV:} & |m_U - m_D| \sim 50 \text{ GeV}, & \chi^2_{\text{min}}/n_{d.o.f.} = 20.6/12 \\
\text{for } m_H = 300 \text{ GeV:} & |m_U - m_D| \sim 75 \text{ GeV}, & \chi^2_{\text{min}}/n_{d.o.f.} = 20.8/12 \\
\text{for } m_H = 500 \text{ GeV:} & |m_U - m_D| \sim 85 \text{ GeV}, & \chi^2_{\text{min}}/n_{d.o.f.} = 21.4/12
\end{array}
$$

Thus we have two lines ($m_U > m_D$ and $m_U < m_D$) in the $(m_U - m_D, m_H)$ space that correspond to the best fit of data. Along these lines the quality of the fit is only slightly better for light higgs ($m_H \sim 120$ GeV) than for the heavy one ($m_H \sim 300$ – 500 GeV).

Note that the $n_{d.o.f}$ is 12, unlike the case of the Standard Model, where it was 13 (ref. [3]). This change occurs because in the present paper m_H is not a fitted, but a fixed parameter (hence 13 becomes 14), while m_N and $m_U - m_D$ are two additional fitted parameters (hence 14 becomes 12). (As is well known, $n_{d.o.f.}$ is equal to the number of experimentally measured observables minus the number of fitted parameters.)

For $m_E = 300$ GeV we have the minimum of χ^2 at $m_U - m_D \simeq 25$ GeV and:

$$
\begin{array}{lll}
\text{for } m_H = 120 \text{ GeV:} & m_N \sim 200 \text{ GeV}, & \chi^2_{\text{min}}/n_{d.o.f.} = 23.0/12 \\
\text{for } m_H = 300 \text{ GeV:} & m_N \sim 170 \text{ GeV}, & \chi^2_{\text{min}}/n_{d.o.f.} = 24.0/12 \\
\text{for } m_H = 500 \text{ GeV:} & m_N \sim 150 \text{ GeV}, & \chi^2_{\text{min}}/n_{d.o.f.} = 24.4/12
\end{array}
$$

Thus, the best fit of the data corresponds to the light $m_E \simeq 100$ GeV and $m_N \simeq 50$ GeV. The significance of light m_N (around 50 GeV) was first stressed in [5]. Increase of m_E leads to the increase of m_N and to fast worsening of χ^2_{min}.

Although inclusion of one extra generation improves the quality of the fit (compare $\chi^2/n_{d.o.f.} = 23.8/13$ for the SM from [3] and $\chi^2_{\text{min}}/n_{d.o.f.} = 20.6/12$ from Fig. 1) it remains pretty poor. The poor quality of the fit is due to 3.3σ discrepancy in $s_l^2 \equiv \sin^2\theta_{\text{eff}}$ extracted from leptonic decays and from $A_{FB}^{b,c}$ [11]. If one multiplies experimental errors of A_{FB}^b and A_{FB}^c by a factor 10, one gets good quality of SM fit [11, 3] but with extremely light higgs, having only a small (few percent) likelihood to be consistent with the lower limit from direct searches. We prove that the fourth generation allows to have higgs as heavy as 500 GeV with a perfect quality of the fit: $\chi^2_{\text{min}}/n_{d.o.f.} = 13/12$, if one uses old NuTeV data (see caption of Fig. 2).

To qualitatively understand the dependence of $m_U - m_D$ on m_H in the case of $m_E = 100$ GeV at $\chi^2_{\rm min}$ let us recall how radiative corrections to the ratio m_W/m_Z and to g_A and $R = g_V/g_A$ (the axial and the ratio of vector and axial couplings of Z-boson to charged leptons) depend on these quantities [6]:

$$\delta V^i \approx \left[- \left(\begin{array}{c} \frac{11}{9}s^2 \\ s^2 \\ s^2 + \frac{1}{9} \end{array} \right) \ln(\frac{m_H}{m_Z})^2 + \frac{4}{3}\frac{(m_U - m_D)^2}{m_Z^2} + \left(\begin{array}{c} \frac{16}{9}s^2 \frac{m_U - m_D}{m_U + m_D} \\ 0 \\ \frac{2}{9}\frac{m_U - m_D}{m_U + m_D} \end{array} \right) \right] \tag{1}$$

where $i = m, A, R$, while $s^2 \simeq 0.23$. Corrections to other observables can be calculated in terms of δV^i. In the vicinity of $\chi^2_{\rm min}$ the third term in brackets is much smaller than the second one. Hence the smallness of the left-right asymmetry of the plots of Figs. 1, 2. Since $\frac{11}{9}s^2 \approx s^2 + \frac{1}{9} \approx s^2$, the increase of m_H is compensated by increase of $|m_U - m_D|$ and we have a valley of $\chi^2_{\rm min}$.

Captions of Figs. 1 and 2 reflect recent change in NuTeV data (from $m_W = 80.26 \pm 0.11$ GeV [12] to $m_W = 80.14 \pm 0.08$ GeV [13]) which results in drastic worsening of the fit even in the presence of the fourth generation.

Thus we see that the 4th family scenario is better than the Standard Model, because the latter can produce good fit only when the mass of the higgs is much lower than the lower limit of LEP II, even when experimental data on heavy quark asymmetries and new NuTeV data are ignored.

Note that originally introduced in [14] parameters S, T, U are not adequate for the above analysis, because they assume that all particles of the fourth generation are much heavier than m_Z, while in our case the best fit corresponds to $m_N \sim m_Z/2$. In the paper [2] modified definitions of S and U were used in order to deal with new particles with masses comparable to m_Z. However, let us stress that both original and modified definitions of S, T and U take into account radiative corrections from the "light" 4th neutrino only approximately, while the threshold effects, that are so important for $m_N \simeq 50$ GeV, can be adequately described in the framework of functions V^i.

In conclusion let us stress that in the framework of SUSY with three generations radiative corrections due to loops with superpartners also shift upward the mass of the higgs in the case of not too heavy squarks (300-400 GeV, see Table 1 in [15]) or light sneutrinos (55-80 GeV, see [16]).

V.N., L.O. and M.V. were partly supported by RFBR grant No. 00-15-96562; V.N. was partly supported by the grant INTAS OPEN 2000-110 as

well. We are grateful to M.Chanowitz for his comments.

References

[1] The LEP Collaborations, the LEPEWWG and the SLD Heavy Flavour and Electroweak working groups, CERN-EP/2001-098, hep-ex/0112021 (2001), Table 13.1.

[2] H.-J. He, N. Polonsky and S. Su, Phys. Rev. **D64** (2001) 053004; hep-ph/0102144.

[3] V.A. Novikov et al., Phys. Lett. **B529** (2002) 111; hep-ph/0111028.

[4] N. Evans, Phys. Lett. **B340** (1994) 81;
Bamert and C.P. Burgess, Z. Phys. **C66** (1995) 495;
T. Inami et al., Mod. Phys. Lett. **A10** (1995) 1471;
Masiero et al., Phys. Lett. **B355** (1995) 329;
V.A. Novikov, L.B. Okun, A.N. Rozanov et al., Mod. Phys. Lett. **A10** (1995) 1915; Erratum - ibid. **A11** (1996) 687;
J. Erler, P. Langacker, Review of Particle Physics. The European Physical Journal **C15** (2000) 95, Chapter 10.6.

[5] M. Maltoni, V.A. Novikov et al., Phys. Lett. **B476** (2000) 107.

[6] V.A. Novikov et al., Rep. on Progr. in Phys. **62** (1999) 1275;
M. Maltoni, Thesis, 1999 (unpublished); hep-ph/0002143.

[7] J.I.Silva-Marcos, hep-ph/0204217; Phys. Rev. **D59** (1999) 091301 (hep-ph/9811381).

[8] V.A. Novikov et al., Preprint ITEP 19-95; preprint CPPM-1-95;
http://cppm.in2p3.fr./leptop/intro_leptop.html.

[9] V.A. Ilyin et al., Phys. Lett. **B503** (2001) 126; hep-ph/0006324.

[10] The ALEPH Collaboration, ALEPH 2001-010; CONF 2001-007 (2001);
P.Abreu et al, DELPHI Collaboration, Eur.Phys.J. C 16 (2000) 53;
M.Acciari et al., L3 Collaboration, Phys.Lett. B470 (1999) 268;
G.Abbiendi et al., OPAL Collaboration, Eur.Phys.J. C 14 (2000) 73;
see also the contributions to the Summer 2001 Conferences.

[11] M.S. Chanowitz, Phys. Rev. Lett. **87** (2001) 231802; hep-ph/0104024.

[12] R.A.Johnson et al., hep-ex/9904028 (1999).

[13] G.P.Zeller et al., hep-ex/0110059 (2001).

[14] M. Peskin and T. Takeuchi, Phys. Rev. Lett. **65** (1990) 964; Phys. Rev. **D46** (1992) 381.

[15] I.V.Gaidaenko et al., Phys.Rep. **320** (1999) 119; hep-ph/9812346.

[16] G.Altarelli et al., JHEP 0106 (2001) 018; hep-ph/0106029.

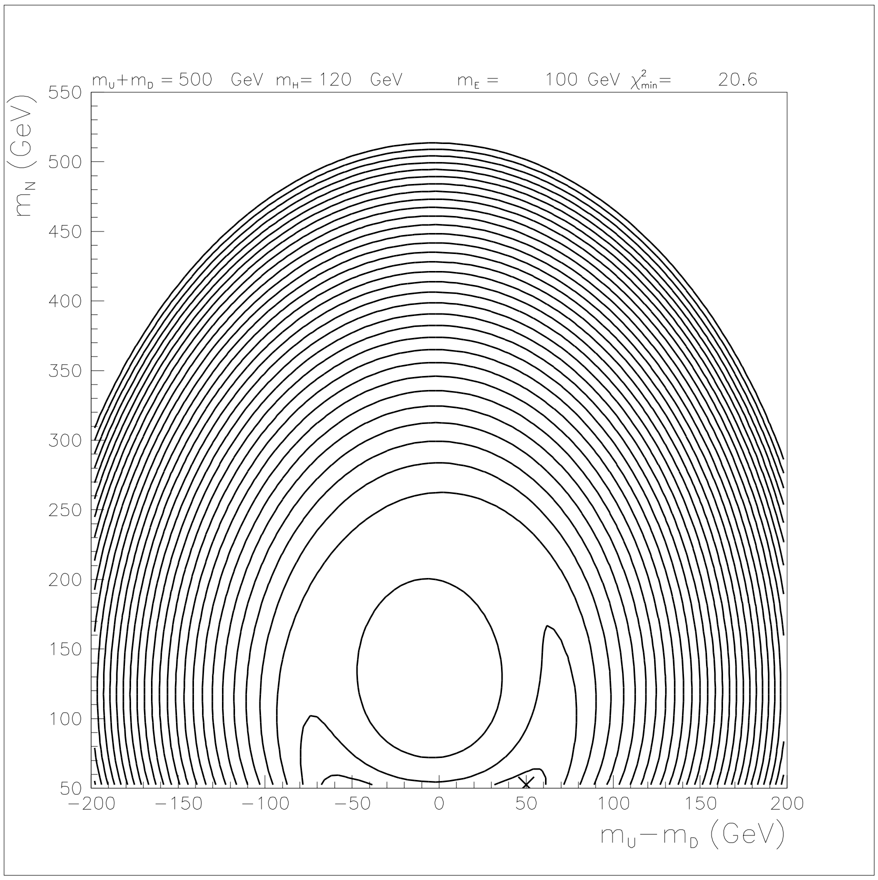

Figure 1: Exclusion plot on the plane $m_N, m_U - m_D$ for fixed values of $m_H = 120$ GeV, $m_U + m_D = 500$ GeV and $m_E = 100$ GeV. $\chi^2_{\rm min}$ shown by two crosses corresponds to $\chi^2/n_{d.o.f.} = 20.6/12$. (The left-hand cross is slightly below $m_N = 50$ GeV.) Borders of regions show domains allowed at the level $\Delta\chi^2 = 1, 4, 9, 16$, etc. The plot was based on the old NuTeV data. The new NuTeV data preserve the pattern of the plot, but lead to $\chi^2_{\rm min}/n_{d.o.f.} = 27.7/12$. If A^b_{FB} and A^c_{FB} uncertainties are multiplied by factor 10 we get $\chi^2_{\rm min}/n_{d.o.f.} = 19.1/12$ for new NuTeV, and $\chi^2_{\rm min}/n_{d.o.f.} = 11.3/12$ for old NuTeV with practically the same pattern of the plot.

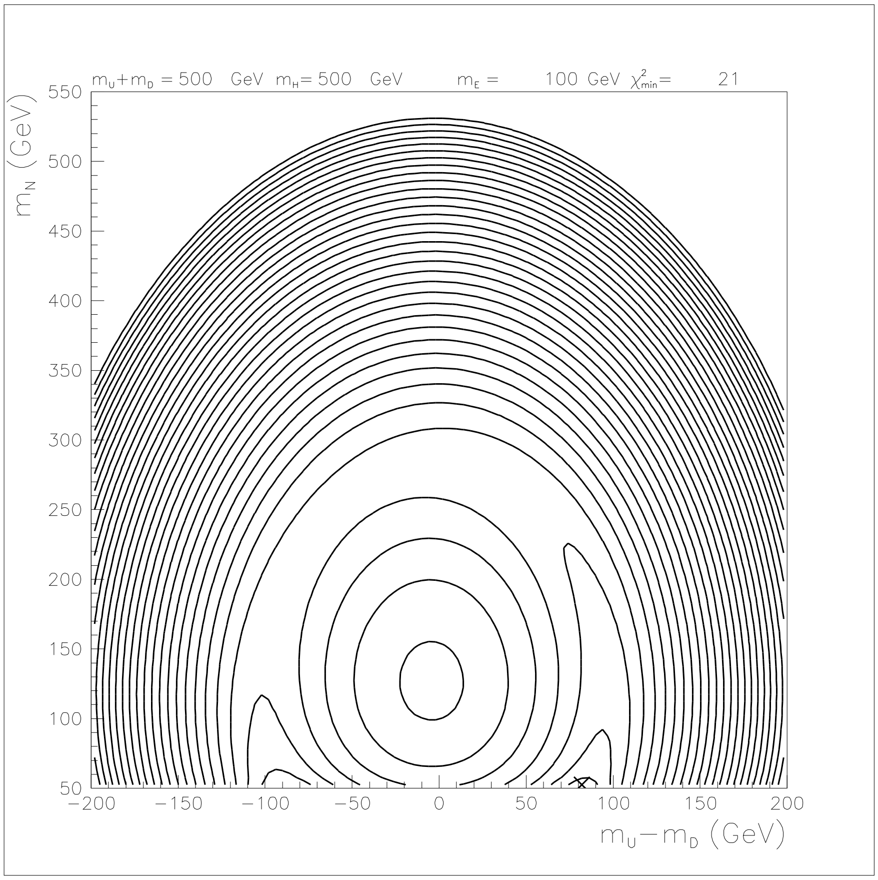

Figure 2: Exclusion plot on the plane $m_N, m_U - m_D$ for fixed values of $m_H = 500$ GeV, $m_U + m_D = 500$ GeV and $m_E = 100$ GeV. $\chi^2_{\rm min}$ shown by two crosses corresponds to $\chi^2/n_{d.o.f.} = 21.4/12$. (The left-hand cross is slightly below $m_N = 50$ GeV.) Borders of regions show domains allowed at the level $\Delta\chi^2 = 1, 4, 9, 16$, etc. The plot was based on the old NuTeV data. The new NuTeV data preserve the pattern of the plot, but lead to $\chi^2_{\rm min}/n_{d.o.f.} = 28.3/12$. If A^b_{FB} and A^c_{FB} uncertainties are multiplied by a factor 10, we get $\chi^2_{\rm min}/n_{d.o.f.} = 21.2/12$ for new NuTeV, and $\chi^2_{\rm min}/n_{d.o.f.} = 13/12$ for old NuTeV with practically the same pattern of the plot.

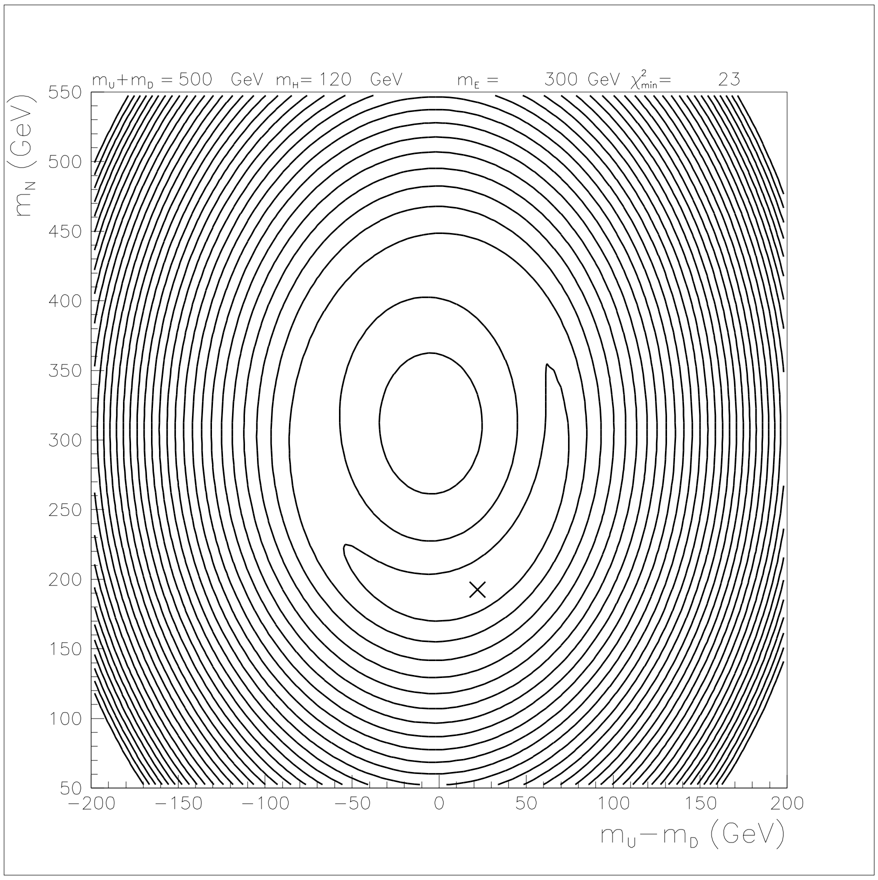

Figure 3: Exclusion plot on the plane $m_N, m_U - m_D$ for fixed values of $m_H = 120$ GeV, $m_U + m_D = 500$ GeV and $m_E = 300$ GeV. $\chi^2_{\rm min}$ shown by cross corresponds to $\chi^2/n_{d.o.f.} = 23.0/12$. Borders of regions show domains allowed at the level $\Delta\chi^2 = 1, 4, 9, 16$, etc.

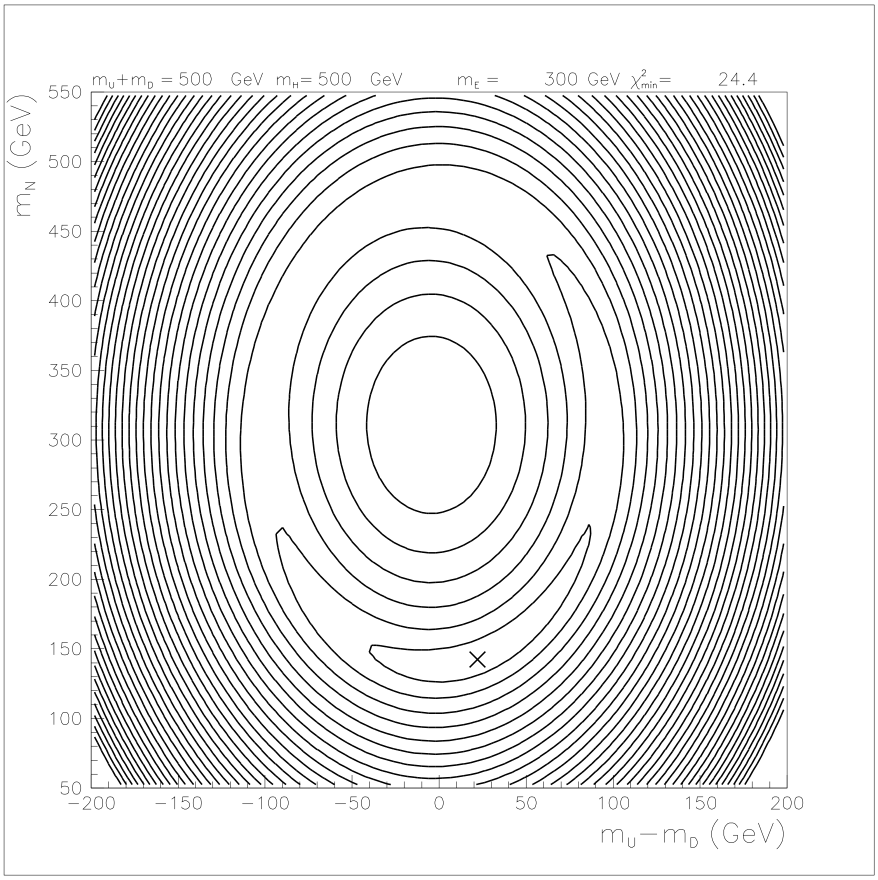

Figure 4: Exclusion plot on the plane $m_N, m_U - m_D$ for fixed values of $m_H = 500$ GeV, $m_U + m_D = 500$ GeV and $m_E = 300$ GeV. $\chi^2_{\rm min}$ shown by cross corresponds to $\chi^2/n_{d.o.f.} = 24.4/12$. Borders of regions show domains allowed at the level $\Delta\chi^2 = 1, 4, 9, 16$, etc.